Micro-Compression of Freestanding Electroplated Copper Through-Glass Vias

Omar Ahmed, Golareh Jalilvand, Chukwudi Okoro, Scott Pollard, and Tengfei Jiang, *Member, IEEE*

***Abstract*—In this study, the micro-compression of freestanding copper (Cu) through-glass vias (TGVs) is presented. An innovative approach was developed to obtain freestanding Cu TGVs where the Cu overburden was used as a bottom platen for the micro-compression test, allowing the mechanical responses of individual TGVs to be directly obtained. From the measured mechanical responses, the average yield strength of the Cu TGVs was determined as 123 MPa with a standard deviation of 7.85MPa. The yield strength values of the six tested TGVs were in good agreement, indicating a reliable and repeatable test procedure. This value was found to be slightly lower than the yield stress values of Cu TSVs, but within the range reported for electroplated Cu. Factors that affect the mechanical properties of the Cu TGVs, including electroplating parameters and microstructure variation, were discussed. The sample preparation and the micro-compression test methods demonstrated in this study can be readily adopted for TGVs subjected to various fabrication and annealing conditions, which will enable the fine-tuning of the processing parameters to produce Cu TGVs with desirable properties for a specific application. Results from this test will also provide valuable input for predictive thermo-mechanical models to enable the development of reliable glass interposers.**

***Index Terms*—Through glass vias, micro-compression testing, mechanical properties, 2.5D interposer.**

I. Introduction

2.5D INTEGRATED circuits (IC), where active dies are placed side-by-side on a passive interposer, is an emerging technology to meet the ever-increasing demands for higher I/O density, increased signal frequency, more functionality, better performance, and smaller footprint in microelectronics [1]–[4]. Glass is a promising substrate material for high performance interposers because of its favorable properties, including the adjustable coefficient of thermal expansion (CTE), dimensional stability, good surface quality, low dielectric constant, low insertion loss, and the compatibility for panel production [5]–[8]. A critical enabling component for glass interposers is the Cu-plated through-glass vias (TGVs), which provides the crucial vertical electrical connections and facilitates heat dissipation [8]–[10]. Cu is widely adopted as the metallization material for TGVs because of its desirable electrical and thermal properties, as well as its compatibility with the existing microelectronics fabrication processes [11], [12]. However, due to the mismatch of coefficient of thermal expansion (CTE) between Cu and glass, thermal stress is generated in and around the TGVs raising reliability concerns such as via extrusion, fracture, and delamination [13], [14]. These stress- induced phenomena can be directly related to the mechanical properties of the electroplated Cu [14]–[16], raising the need to characterize the mechanical properties of Cu TGVs. Obtaining the properties of Cu TGVs is also important for the development and implementation of models to analyze the thermo-mechanical reliability, optimize design and predict reliability for glass-based interposers.

Two techniques are commonly used to characterize the mechanical behaviors of a small volume of materials: nanoindentation and micro-compression [17]–[23]. Nanoindentation has many advantages including the ease of use, location specificity, and high displacement and load resolutions [17], [18], but its accuracy is affected by the shape and sharpness of the nanoindentation tip [24]–[26]. Additional analysis, such as by finite element analysis (FEA), is needed to extract the plastic properties of the materials based on the load-displacement curves using an iterative process [27]–[29], but the data analysis is complicated by the complex stress state underneath the indentation tip [30], [31]. In comparison, the micro-compression test applies a nominally uniaxial loading on the sample, which is advantageous for the testing of a wide range of materials that are difficult to test in the bulk form [24]. Samples used in the micro-compression test are usually pillars fabricated from the bulk of the material by focused ion beam (FIB) milling, a process that may affect the mechanical response of the material due to damages by ion beam irradiation [20], [22], [32]–[34]. While both nanoindentation and micro-compression have been used to characterize the mechanical behaviors of Cu TSVs [11], [12], [35]–[37], no such studies have been reported for Cu TGVs. The differences in the dimension, fabrication process, and substrate materials between the TGVs and TSVs imply that the mechanical behaviors of TGVs may be different from those of TSVs,

Manuscript received December 4, 2019; revised February 3, 2020; accepted February 10, 2020. Date of publication February 13, 2020; date of current version March 6, 2020. This work was supported by NSF I/UCRC on Multi-Functional Integrated System Technology (MIST) Center under Grant IIP-1439644, Grant IIP-1439680, and Grant IIP-1738752. *(Corresponding author: Omar Ahmed.)*

Omar Ahmed, Golareh Jalilvand, and Tengfei Jiang are with the Department of Materials Science and Engineering, University of Central Florida, Orlando, FL 32816 USA (e-mail: omar.s.ahmed@knights.ucf.edu; tengfei.jiang@ucf.edu).

Chukwudi Okoro is with the Department of Mechanics and Reliability Sciences, Corning Research and Development Corporation, Corning, NY 14831 USA.

Scott Pollard is with the Department of Integration Technologies, Corning Research and Development Corporation, Corning, NY 14831 USA.

Color versions of one or more of the figures in this article are available online at http://ieeexplore.ieee.org.

Digital Object Identifier 10.1109/TDMR.2020.2973940

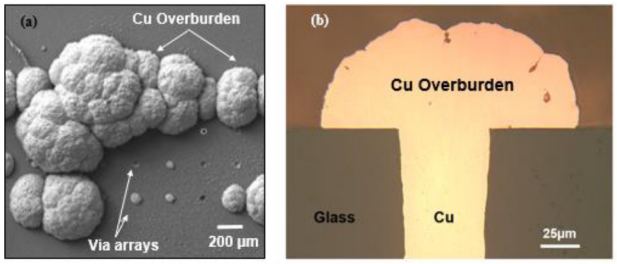

Fig. 1. (a) An SEM top view image of a typical TGV array showing the vias and the Cu overburden. (b) A zoomed-in cross-sectional optical image showing the Cu overburden at the top of the via.

raising the need to characterize the mechanical properties of TGVs.

In this work, micro-compression test was carried out on freestanding Cu TGVs. A novel sample preparation method was developed to fabricate the freestanding Cu TGV pillars without FIB milling, therefore avoiding the adverse effect of ion beam damage on the measured properties. From the acquired stress-strain curve, the yield strength of the Cu TGVs was obtained, which will provide valuable input for numerical models for the assessment of stress and reliability in TGV-containing structures. This paper is organized as the follows. First, experimental details on the sample preparation method were given. Next, the micro-compression test and the procedures to convert the measured load-displacement curves to stress-strain curves were described. Finally, the results obtained from the test were presented and discussed

II. Experimental Details

A. Preparation of the Free-Standing TGVs Pillars

The Cu TGVs used in this study were fabricated using a previously described process [38] where via holes in a glass wafer were filled by Cu electroplating. The via diameters were 50 µm and the wafer thickness was 365 µm. Post-plating annealing was carried out at 420°C for 30 minutes and no chemical-mechanical planarization (CMP) was performed. Fig. 1a is a top-view scanning electron microscope (SEM) image of a TGV coupon showing an array of vias, and Fig. 1b is a cross-sectional optical image near the top of the via. Overburden, which is the excessive Cu deposited at the top of the vias, can be seen in both images and have the shape of mushrooms.

Taking advantage of the presence of the Cu overburdens, a procedure was developed to create the freestanding Cu TGV pillars for the micro-compression test, as illustrated in Fig. 2. First, rectangular coupons that were 20 mm × 10 mm in size were cut from the TGV wafer (Fig. 2a) and placed in a mounting mold. The coupons were then potted in epoxy and allowed to cure at room temperature for 24 hours (Fig. 2b). The sample, which now consisted of the TGV coupon embedded in the hardened epoxy, was flipped upside down and polished from the bottom side until the height of the vias was reduced to between 30-50 µm (Fig. 2c). Next, HF was used to selectively etch off the glass substrate and expose the Cu vias (Fig. 2d). The sample was ultrasonically cleaned in ethanol to remove any residue from the glass etching process.

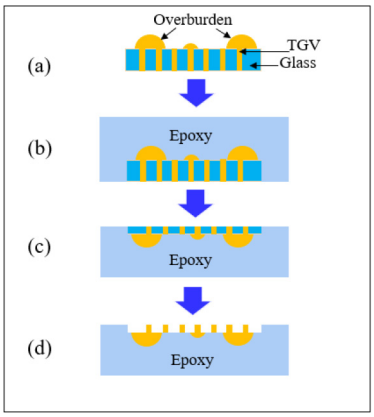

Fig. 2. Schematic illustrations of the procedure used to obtain the freestanding Cu TGVs. (a) A cross-sectional view of the as-received TGV coupon showing the embedded vias and the Cu overburden. (b) The TGV coupon was mounted in epoxy and allowed to cure at room temperature for 24 hours. (c) The TGV coupon was flipped and thinned down from the bottom side of the coupon until the via height was between 30-50µm. (d) Glass was removed by etching with HF to expose the freestanding TGV pillars.

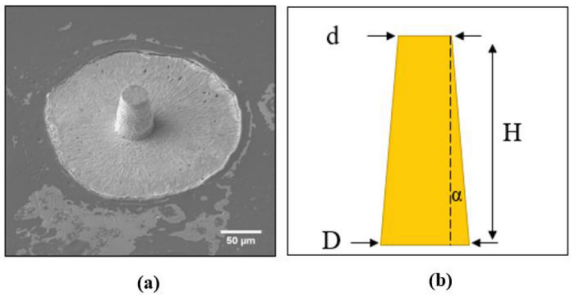

Fig. 3. (a) SEM image of a freestanding TGV prepared by the method presented in Fig. 2. (b) An illustration of the geometrical parameters used to describe the TGV pillars. D is the diameter at the base of the pillar, d is the diameter at the top of the pillar, H is the height of the pillar, and α is the tapering angle.

Energy dispersive spectroscopy (EDS) was carried out and confirmed that glass had been completely removed and pristine freestanding Cu TGVs had been obtained by the described procedure. Studies have shown that Cu experiences minimal (100-500Å) to no corrosion from exposure to aqueous HF solutions [39]–[41]. Therefore, the method described above, which utilizes the overburden as a bottom platen to support the TGV pillars, allowed pristine freestanding vias to be obtained for the subsequent micro-compression testing.

The SEM image of a typical freestanding Cu TGV pillars prepared by this method is shown in Fig. 3. The via, now in the form of a pillar, was situated on top of its original overburden, which served as a bottom platen to provide the structural support during the uniaxial micro-compression test. As illustrated in Fig. 3b, four geometrical parameters were used to describe the geometry of the via pillar. D refers to the diameter of the via at base, d (<D) refers to the diameter at the top of the via, which is also the free end, H refers to the height of the via, and α is the tapering angle between the tangent of the via sidewall surface and the via axis. Six freestanding TGV pillars were obtained in a coupon and were used for the micro-compression test. Prior to being tested, each via was examined in SEM and the geometry parameters were determined from

TABLE I
THE DIMENSIONS OF THE TGV PILLARS TESTED IN THIS STUDY

Via #	D (μm)	d (μm)	H (μm)	α (°)
1	50	49	33.62	0.85
2	50	47	44.55	1.92
3	50	47.6	49.81	1.37
4	50	49.2	43.74	0.52
5	50	47.2	44.96	1.87
6	50	49.0	38.07	0.75

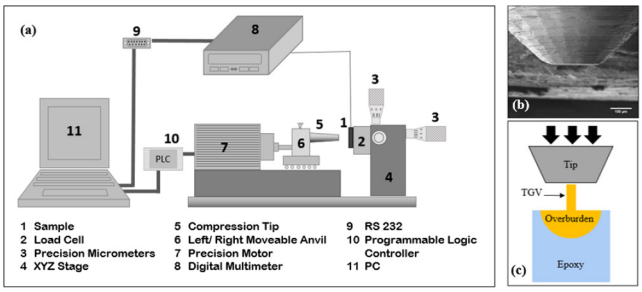

Fig. 4. (a) Illustration of the micro-compression setup used in this study. (b) An SEM image of the micro-compression tip. (c) A schematic illustration of the testing procedure for the micro-compression of TGV pillars.

the SEM image using the image analysis tool, Image J. The dimensions of these six vias are summarized in Table I.

B. The Micro-Compression Test

Uniaxial micro-compression tests were carried out using a setup illustrated in Fig. 4a. The test system consisted of a precision motor, a load cell, a stereoscope, a side view camera, and precision micrometers, and was controlled by a closed-loop LabView data acquisition program. For each micro-compression test, the sample, which contained the free-standing TGV pillars, was attached to the load cell. The pillar to be tested was first located by the stereoscope and the side view camera, and then aligned and centered with the micro-compression tip. Fine alignment of the pillar to the tip was achieved by the precision micrometers that were attached to the load cell. Fig. 4b is the SEM image of the flat-top steel tip used in the tests, which had a diameter of 200 μm. As shown in Fig. 4c, during the test, a LabView-based program was used to control the movement of the precision motor, which pushed the micro-compression tip towards the sample at a speed of 50 nm/sec. The TGV pillar was compressed in a uniaxial fashion with the via overburden served as the bottom platen. The compressive force imposed by the tip on the TGV pillar was measured by the load cell, which has a minimum force resolution of ±1 mN. The load-displacement response of each via was recorded in real time as the test was being conducted by the LabView-based program for further analysis.

After the micro-compression tests, the load-displacement plots were obtained, which were then converted to stress-strain plots for the tested vias. The total compliance measured from the test was the sum of the compliance of the test system, the compliance of the TGV pillar, and the compliance of the base supporting the pillar [23]:

$$C_{total} = C_{sys} + C_{via} + C_{base} \tag{1}$$

where the subscripts *sys*, *via*, and *base* refer to the test system, the via, and the Cu overburden, respectively. The compliance of the test system was obtained by calibration using a material with a known compliance before the testing. The compliance of the base was associated with the "sink in" of the Cu overburden during the test, which can be obtained using the analysis by Sneddon [24], [42], [43] as:

$$C_{base} = \frac{\sqrt{\pi}\left(1-\nu^2\right)}{2E\sqrt{A}} \tag{2}$$

where ν and E are the Poisson's ratio and Young's modulus of the Cu overburden, respectively. A is the contact area between the pillar and the overburden, $A = \frac{\pi D^2}{4} = \pi r_{base}^2$, where D is the diameter of the base, as shown in Fig. 3, and r_{base} is the radius of the pillar at the base, $r_{base} = \frac{D}{2}$.

The displacement of the via can be calculated as:

$$\Delta X_{via} = \Delta x_{total} - \left(C_{sys} + C_{base}\right)f \tag{3}$$

where f is the force measured by the load cell and Δx_{total} is the total displacement.

The pillar strain can then be calculated as:

$$\text{Strain}_{(TGV)} = \frac{\Delta X_{via}}{H_{via}} \tag{4}$$

where H is the TGV length measured from the SEM image, as shown in Fig. 3.

To calculate the stress in each TGV, the variation in the TGV diameter is considered in an empirical equation to average the non-uniformity in the stress field. The following expression is used [25]:

$$\sigma = \frac{1}{2}\left(\frac{r_{ind}^2}{r_{top}^2} + \frac{r_{ind}^2}{r_{base}^2}\right).p \tag{5}$$

where r_{ind}, r_{top}, and r_{base} stand for the indenter radius, the via top radius, and the via base radius, respectively. P is the pressure = applied load /indenter area.

III. EXPERIMENTAL RESULTS AND DISCUSSION

The six freestanding TGV pillars described in Table I were compressed using the displacement-controlled mode with a prescribed displacement speed of 50 nm/s. All pillars were compressed to 30% of their original length (H) to obtain their stress-strain responses. Fig. 5 shows the stress-strain curves of all the six TGVs tested in this study. From the stress-strain curves, the 0.2% proof strength was determined as the yield strength of the tested vias, which were summarized in Table II. The average yield strength was found to be 123 MPa with a standard deviation of 7.85MPa. The yield strength values of the six tested TGVs were in good agreement, indicating a reliable and repeatable test procedure. The variation of the measured yield strength and the stress-strain curves among the vias may be related to the stochastic variations of the microstructure, the tapering angles, and the presence of a small number of voids in the via.

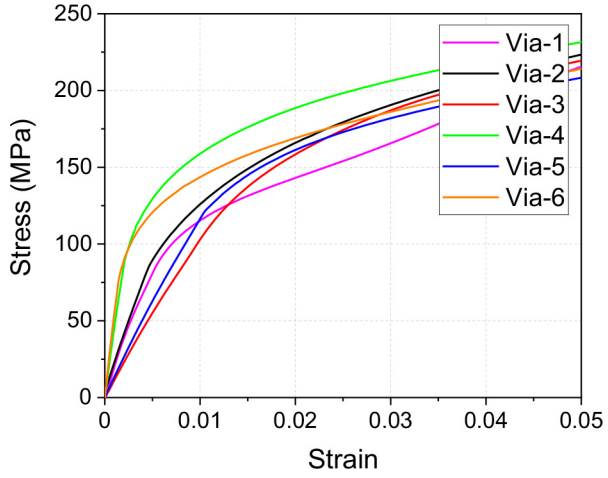

Fig. 5. The Stress-Strain curves of all the six vias tested in this study.

TABLE II
0.2% YIELD STRENGTH VALUES

Via #	0.2 % Yield Strength (MPa)
1	113
2	115
3	130
4	125
5	135
6	120

This work marks the first time that the yield strength of TGVs was determined experimentally. The yield strength value of 123 MPa falls within the range of values reported for electroplated Cu film [44]–[46] but is lower than the value of 167 MPa obtained by micro-compression for electroplated Cu TSVs [21]. Okoro *et al.* [47] has shown that the plastic properties of Cu vias used as the input in a numerical model has a direct impact on the predicted stress levels in the surrounding Si substrate. The observed difference in yield strength values, especially between TGVs and TSVs, underscores the importance to characterize the mechanical properties of TGVs for the reliability analysis of TGV-based applications.

Several factors can cause the observed differences in yield strength between Cu TGVs and the other structures such as thin films and TSVs, including the electroplating chemistries, geometry of the structure, and the resulting Cu microstructure [45], [48]–[54]. The sample preparation method to isolate freestanding TGVs and the micro-compression testing procedures described in this study provide an important avenue for the investigation of processing and microstructural parameters on the mechanical properties and reliability of TGVs. For example, measurements can be carried out on a series of TGVs that are fabricated by various processing parameters to reveal the effect of processing on the mechanical properties of TGVs. Fine-tuning of the processing parameters can subsequently be made, for example, by modifications of electroplating chemistry [50], [51], [55] to achieve TGV with desirable mechanical properties. Studies on the effects of processing and microstructural factors on the mechanical behaviors of Cu TGVs will be the subject of future studies.

IV. CONCLUSION

Micro-compression of freestanding Cu TGVs was conducted in this study. Although several studies exist on the characterization of mechanical properties of Cu TSVs, this is the first time that the mechanical properties of Cu TGVs are reported. Comparing to the nanoindentation technique, micro-compression has the advantage of subjecting the sample to nominal uniaxial loading, allowing easy interpretation of the test data to obtain the yield strength of the material. A novel sample preparation procedure was developed to fabricate freestanding Cu TGV pillars by taking advantage of the presence of the overburden. Six Cu TGVs were tested and the average yield strength was determined as 123 MPa. This value was found to be slightly lower than the yield stress values of Cu TSVs, but within the range reported for electroplated Cu. This difference may be traced to various electroplating parameters and microstructure that affect the properties of the vias. The sample preparation procedure and test method presented in this work provide a viable and reliable method to examine the mechanical properties of TGVs by micro-compression.

REFERENCES

[1] K. Demir *et al.*, "Thermomechanical and electrochemical reliability of fine-pitch through-package-copper vias (TPV) in thin glass interposers and packages," in *Proc. IEEE 63rd Electron. Compon. Technol. Conf.*, 2013, pp. 353–359.
[2] A. Horibe *et al.*, "Through silicon via process for effective multi-wafer integration," in *Proc. IEEE 65th Electron. Compon. Technol. Conf. (ECTC)*, 2015, p. 1808.
[3] D. Malta *et al.*, "Fabrication of TSV-based silicon interposers," in *Proc. IEEE Int. 3D Syst. Integr. Conf. (3DIC)*, 2010, pp. 1–6.
[4] T. Lenihan, L. F. Matthew, and E. J. Vardaman, "Developments in 2.5D: The role of silicon interposers," in *Proc. IEEE 15th Electron. Packag. Technol. Conf. (EPTC)*, 2013, pp. 53–55.
[5] S. Cho, Y. K. Joshi, V. Sundaram, Y. Sato, and R. R. Tummala, "Comparison of thermal performance between glass and silicon interposers," in *Proc. IEEE 63rd Electron. Compon. Technol. Conf.*, 2013, pp. 1480–1487.
[6] V. Sukumaran *et al.*, "Design, fabrication, and characterization of ultra-thin 3-D glass interposers with through-package-vias at same pitch as TSVs in silicon," *IEEE Trans. Compon. Packag. Manuf. Technol.*, vol. 4, no. 5, pp. 786–795, May 2014.
[7] J. Keech, G. Piech, S. Pollard, S. Chaparala, A. Shorey, and B. K. Wang, "Glass interposer substrates: Fabrication, characterization and modeling," in *Proc. IEEE 15th Electron. Packag. Technol. Conf. (EPTC)*, 2013, pp. 1–23.
[8] M. Lueck, A. R. Huffman, and A. B. Shorey, "Through glass vias (TGV) and aspects of reliability," in *Proc. IEEE 65th Electron. Compon. Technol. Conf. (ECTC)*, 2015, pp. 672–677.
[9] C.-H. Chien *et al.*, "Performance and process comparison between glass and Si interposer for 3D-IC integration," in *Proc. Int. Symp. Microelectron.*, 2013, pp. 618–624.
[10] A. B. Shorey and R. Lu, "Progress and application of through glass via (TGV) technology," in *Proc. Pan Pac. Microelectron. Symp. (Pan Pacific)*, 2016, pp. 1–6.
[11] O. Chukwudi *et al.*, "Influence of annealing conditions on the mechanical and microstructural behavior of electroplated Cu-TSV," *J. Micromechan. Microeng.*, vol. 20, no. 4, 2010, Art. no. 045032.
[12] A. Heryanto *et al.*, "Effect of copper TSV annealing on via protrusion for TSV wafer fabrication," *J. Electron. Mater.*, vol. 41, no. 9, pp. 2533–2542, 2012.
[13] S.-K. Ryu, K.-H. Lu, X. Zhang, J.-H. Im, P. S. Ho, and R. Huang, "Impact of near-surface thermal stresses on interfacial reliability of through-silicon vias for 3-D interconnects," *IEEE Trans. Device Mater. Rel.*, vol. 11, no. 1, pp. 35–43, Mar. 2011.

[14] D. Zhang, K. Hummler, L. Smith, and J. J.-Q. Lu, "Backside TSV protrusion induced by thermal shock and thermal cycling," in *Proc. IEEE 63rd Electron. Compon. Technol. Conf.*, 2013, pp. 1407–1413.

[15] S.-K. Ryu *et al.*, "Characterization of thermal stresses in through-silicon vias for three-dimensional interconnects by bending beam technique," *Appl. Phys. Lett.*, vol. 100, no. 4, 2011, Art. no. 041901.

[16] T. Jiang, S.-K. Ryu, Q. Zhao, J. Im, R. Huang, and P. S. Ho, "Measurement and analysis of thermal stresses in 3D integrated structures containing through-silicon-vias," *Microelectron. Rel.*, vol. 53, no. 1, pp. 53–62, 2013.

[17] W. C. Oliver and G. M. Pharr, "An improved technique for determining hardness and elastic modulus using load and displacement sensing indentation experiments," *J. Mater. Res.*, vol. 7, no. 6, pp. 1564–1583, 2011.

[18] X. Li and B. Bhushan, "A review of nanoindentation continuous stiffness measurement technique and its applications," *Mater. Characterization*, vol. 48, no. 1, pp. 11–36, 2002.

[19] L. Jiang and N. Chawla, "Mechanical properties of Cu6Sn5 intermetallic by micropillar compression testing," *Scripta Materialia*, vol. 63, no. 5, pp. 480–483, 2010.

[20] T. Hirouchi and Y. Shibutani, "Mechanical responses of copper bicrystalline micro pillars with Σ 3 coherent twin boundaries by uniaxial compression tests," *Mater. Trans.*, vol. 55, no. 1, pp. 52–57, 2014.

[21] T. Gu, P. Cheng, H. Y. Wang, X. H. Dai, H. Wang, and G. F. Ding "Micro-compression testing of TSV copper pillar: An in situ method and mechanical property," *Adv. Mater. Res.*, vol. 663, pp. 352–356, Feb. 2013.

[22] M. D. Uchic, P. A. Shade, and D. M. Dimiduk, "Micro-compression testing of FCC metals: A selected overview of experiments and simulations," *JOM*, vol. 61, no. 3, pp. 36–41, 2009.

[23] D. R. P. Singh, N. Chawla, G. Tang, and Y.-L. Shen, "Micropillar compression of Al/SiC nanolaminates," *Acta Materialia*, vol. 58, no. 20, pp. 6628–6636, 2010.

[24] H. Zhang, B. E. Schuster, Q. Wei, and K. T. Ramesh, "The design of accurate micro-compression experiments," *Scripta Materialia*, vol. 54, no. 2, pp. 181–186, 2006.

[25] H. Fei, A. Abraham, N. Chawla, and H. Jiang, "Evaluation of micro-pillar compression tests for accurate determination of elastic-plastic constitutive relations," *J. Appl. Mech.*, vol. 79, no. 6, pp. 1–9, 2012.

[26] D. Kiener, C. Motz, and G. Dehm, "Micro-compression testing: A critical discussion of experimental constraints," *Mater. Sci. Eng. A*, vol. 505, no. 1, pp. 79–87, 2009.

[27] A. Karimzadeh, M. R. Ayatollahi, and M. Alizadeh, "Finite element simulation of nano-indentation experiment on aluminum 1100," *Comput. Mater. Sci.*, vol. 81, pp. 595–600, Jan. 2014.

[28] M. Dao, N. Chollacoop, K. J. Van Vliet, T. A. Venkatesh, and S. Suresh, "Computational modeling of the forward and reverse problems in instrumented sharp indentation," *Acta Materialia*, vol. 49, no. 19, pp. 3899–3918, 2001.

[29] J. A. Knapp, D. M. Follstaedt, J. C. Barbour, and S. M. Myers, "Finite-element modeling of nanoindentation for determining the mechanical properties of implanted layers and thin films," *Nucl. Instrum. Methods Phys. Res. B Beam Interact. Mater. Atoms*, vols. 127–128, pp. 935–939, May 1997.

[30] M. E. Barbary, L. Chen, Y. Liu, F. Qin, and X. Fan, "On the uniqueness and sensitivity of nanoindentation testing for determining elastic and plastic material properties of electroplating copper filled in through-silicon-via (TSV)," in *Proc. IEEE 68th Electron. Compon. Technol. Conf. (ECTC)*, 2018, pp. 1023–1029.

[31] S. W. Moore, M. T. Manzari, and Y.-L. Shen, "Nanoindentation in elasto-plastic materials: Insights from numerical simulations," *Int. J. Smart Nano Mater.*, vol. 1, no. 2, pp. 95–114, 2010.

[32] T. Nagoshi, A. Shibata, Y. Todaka, T. Sato, and M. Sone, "Mechanical behavior of a microsized pillar fabricated from ultrafine-grained ferrite evaluated by a microcompression test," *Acta Materialia*, vol. 73, pp. 12–18, Jul. 2014.

[33] C. J. Lee, J. C. Huang, and T. G. Nieh, "Sample size effect and microcompression of Mg65Cu25Gd10 metallic glass," *Appl. Phys. Lett.*, vol. 91, no. 16, 2007, Art. no. 161913.

[34] J. Hütsch and E. T. Lilleodden, "The influence of focused-ion beam preparation technique on microcompression investigations: Lathe vs. annular milling," *Scripta Materialia*, vol. 77, pp. 49–51, Apr. 2014.

[35] P. Dixit, L. Xu, J. Miao, J. H. L. Pang, and R. Preisser, "Mechanical and microstructural characterization of high aspect ratio through-wafer electroplated copper interconnects," *J. Micromechan. Microeng.*, vol. 17, no. 9, p. 1749, 2007.

[36] T. Gu *et al.*, "Mechanical property evaluation of TSV-Cu micropillar by compression method," *Electron. Mater. Lett.*, vol. 10, no. 4, pp. 851–855, 2014.

[37] Y. Song, R. Abbaspour, M. S. Bakir, and S. K. Sitaraman, "Thermal annealing effects on copper microstructure in through-silicon-vias," in *Proc. 15th IEEE Intersociety Conf. Thermal Thermomech. Phenom. Electron. Syst. (ITherm)*, 2016, pp. 91–95.

[38] A. Shorey *et al.*, "Advancements in fabrication of glass interposers," in *Proc. IEEE 64th Electron. Compon. Technol. Conf. (ECTC)*, 2014, pp. 20–25.

[39] R. Hanestad, J. W. Butterbaugh, A. Ben-Hamida, and I. Gelmi, "Stiction-free release etch with anhydrous HF/water vapor processes," in *Proc. SPIE*, 2001, p. 4557.

[40] G. C. whitaker, "Corrosion of metals in fluorine and hydrofluoric acid," *Corrosion*, vol. 6, no. 9, pp. 283–285, 1950.

[41] T. McKenzie, "Thin film resistance to hydrofluoric acid etch with applications in monolithic microelectronic/MEMS integration," M.S. thesis, School Elect. Comput. Eng., Georgia Inst. Technol., Atlanta, GA, USA, 2019.

[42] I. N. Sneddon, "The relation between load and penetration in the axisymmetric boussinesq problem for a punch of arbitrary profile," *Int. J. Eng. Sci.*, vol. 3, no. 1, pp. 47–57, 1965.

[43] A. Bharathula, S.-W. Lee, W. J. Wright, and K. M. Flores, "Compression testing of metallic glass at small length scales: Effects on deformation mode and stability," *Acta Materialia*, vol. 58, no. 17, pp. 5789–5796, 2010.

[44] Y. Xiang, T. Y. Tsui, and J. J. Vlassak, "The mechanical properties of freestanding electroplated Cu thin films," *J. Mater. Res.*, vol. 21, no. 6, pp. 1607–1618, 2006.

[45] S. Zhang, M. Sakane, T. Nagasawa, and K. Kobayashi, "Mechanical properties of copper thin films used in electronic devices," *Procedia Eng.*, vol. 10, pp. 1497–1502, Jun. 2011.

[46] Y. Xiang, X. Chen, and J. Vlassak, "The mechanical properties of electroplated Cu thin films measured by means of the bulge test technique," in *Proc. MRS*, 2001. p. 695.

[47] C. Okoro *et al.*, "Extraction of the appropriate material property for realistic modeling of through-silicon-vias using μ-Raman spectroscopy," in *Proc. Int. Interconnect Technol. Conf.*, 2008, pp. 16–18.

[48] A. Ibañez and E. Fatás, "Mechanical and structural properties of electrodeposited copper and their relation with the electrodeposition parameters," *Surface Coatings Technol.*, vol. 191, no. 1, pp. 7–16, 2005.

[49] J. B. Marro, T. Darroudi, C. A. Okoro, Y. S. Obeng, and K. C. Richardson, "The influence of pulse plating frequency and duty cycle on the microstructure and stress state of electroplated copper films," *Thin Solid Films*, vol. 621, pp. 91–97, Jan. 2017.

[50] J. B. Marro, T. Darroudi, C. A. Okoro, Y. S. Obeng, and K. C. Richardson, "The influence of pulsed electroplating frequency and duty cycle on copper film microstructure and stress state," *Thin Solid Films*, vol. 621, pp. 91–97, Jan. 2017.

[51] J. B. Marro, C. A. Okoro, Y. S. Obeng, and K. C. Richardsona, "The impact of organic additives on copper trench microstructure," *J. Electrochem. Soc.*, vol. 164, no. 9, pp. D543–D550, 2017.

[52] X. Feng, W. Luo, M. Li, and S. Wang, "Effect of leveler on microstructure and stress of electroplated copper for TSV application," in *Proc. 3rd IEEE CPMT Symp. Japan*, 2013, pp. 1041–1048.

[53] C. Okoro *et al.*, "Impact of the electrodeposition chemistry used for TSV filling on the microstructural and thermo-mechanical response of Cu," *J. Mater. Sci.*, vol. 46, no. 11, pp. 3868–3882, 2011.

[54] D.-H. Jung *et al.*, "Effect of current density and plating time on Cu electroplating in TSV and low alpha solder bumping," *J. Mater. Eng. Perform.*, vol. 24, no. 3, pp. 1107–1115, 2015.

[55] J. Marro, "Tunable copper microstructures in blanket films and trenches using pulsed electrodeposition," in *Proc. Mater. Sci. Eng.*, 2016, p. 239.